

NASACR-177,988

NASA Contractor Report 177988

ICASE REPORT NO. 85-43

NASA-CR-177988
19860004485

ICASE

ACCURACY OF SCHEMES WITH NONUNIFORM MESHES
FOR COMPRESSIBLE FLUID FLOWS

Eli Turkel

NASA Contract No. NAS1-17070
September 1985

LIBRARY COPY

NOV 14 1985

LANGLEY RESEARCH CENTER
LIBRARY, NASA
HAMPTON, VIRGINIA

INSTITUTE FOR COMPUTER APPLICATIONS IN SCIENCE AND ENGINEERING
NASA Langley Research Center, Hampton, Virginia 23665

Operated by the Universities Space Research Association

NASA

National Aeronautics and
Space Administration

Langley Research Center
Hampton, Virginia 23665



NF01014

ACCURACY OF SCHEMES WITH NONUNIFORM MESHES
FOR COMPRESSIBLE FLUID FLOWS

Eli Turkel
Tel-Aviv University
and
Institute for Computer Applications in Science and Engineering

Abstract

We consider the accuracy of the space discretization for time-dependent problems when a nonuniform mesh is used. We show that many schemes reduce to first-order accuracy while a popular finite volume scheme is even inconsistent for general grids. This accuracy is based on physical variables. However, when accuracy is measured in computational variables then second-order accuracy can be obtained. This is meaningful only if the mesh accurately reflects the properties of the solution. In addition we analyze the stability properties of some improved accurate schemes and show that they also allow for larger time steps when Runge-Kutta type methods are used to advance in time.

Research was supported in part by the National Aeronautics and Space Administration under NASA Contract No. NAS1-17070 while the author was in residence at ICASE, NASA Langley Reserach Center, Hampton, VA 23665.

I. INTRODUCTION

With the latest class of computers it is now possible to routinely perform two-dimensional calculations for both the Euler and the compressible Navier-Stokes equations. Three-dimensional Euler calculations about simple shapes are feasible if a relatively coarse grid is used. Three-dimensional calculations based on the thin layer compressible Navier-Stokes calculations are just becoming available. The current trend is to use coordinates constructed so that the solid surfaces are coordinate lines while the other coordinate directions are close to orthogonal (see however [4]). This approach simplifies the boundary conditions at the solid surfaces. Moreover, whenever boundary layers exist, this approach allows one to refine the mesh across the boundary layer while having a relatively coarse mesh parallel to the boundary layer.

The construction of a general curvilinear grid is still not easily accomplished. Difficulties occur when one wishes the grids to vary smoothly while also being able to concentrate points in certain regions. Since many bodies have cusped regions, the meshes frequently are far from regular in these regions. In three dimensions these difficulties are compounded. First, on present day machines one is still restricted to relatively coarse grids. In addition the shape of the bodies can be more complicated in three dimensions. One frequently uses a quasi two-dimensional approach which has difficulties when the body no longer appears in some two-dimensional slice. The result of all these difficulties is that the meshes that are constructed are highly distorted in some regions. These distortions appear as high aspect ratios and angles quite far from 90° for quadrilateral elements. Even more disturbing is the change of these quantities from a cell to its neighboring cells (see, for example, Figure 2).

In this paper we consider two aspects of the calculations for compressible flow. The first is the accuracy of various schemes when used on grids which have distorted meshes. In addition we shall also consider some explicit time marching techniques that utilize improved space discretizations. We shall also discuss finite volume approaches and show that some of the improvements also allow larger time steps.

The effect of nonuniform grids on accuracy has previously been discussed by several authors, e.g., Hoffman [7], Mastin [9], Steger [14], and Vinokur [22]. Rai et. al. [12] have performed calculations on discontinuous grids using a first-order upwind scheme. Pike [10] has also considered upwind schemes on general (one-dimensional) meshes and has examined conservation and TVD properties.

II. SPACE DISCRETIZATION

We shall consider time dependent problems. This also applies to steady state problems if we use pseudo time-dependent methods. Thus we shall march a time-dependent equation which need not be consistent with the time-dependent physics of the process but has the same steady state equation.

We consider the conservation equations

$$w_t + f_x + g_y + h_z = 0. \quad (2.1)$$

We decouple the time integration from the space discretization. Hence we will, for now, keep the time variable continuous and only consider the approximation in space. Using a finite volume approach we integrate (2.1) in a cell Ω and assuming that Ω is independent of time we obtain

$$\frac{\partial}{\partial t} \int_{\Omega} w dx dy dz + \int_{\Omega} (f_x + g_y + h_z) dx dy dz = 0 \quad (2.2)$$

Using the divergence theorem this becomes

$$\frac{d}{dt} \int_{\Omega} w dV + \int_{\partial\Omega} \vec{F} \cdot \vec{n} dS = 0 \quad (2.3)$$

where $F = (f, g, h)^t$ and n is the unit outward normal. Equivalently,

$$\frac{d}{dt} \left[\frac{\int_{\Omega} w dv}{\int_{\Omega} dv} \right] + \frac{1}{V} \int_{\partial\Omega} \vec{F} \cdot \vec{n} dS = 0. \quad (2.4)$$

Let \bar{w} be the average of w in a cell. Then we have

$$\bar{w} = \frac{1}{V} \int_{\Omega} w dv \quad (2.5a)$$

and

$$\frac{d\bar{w}}{dt} + \frac{1}{V} \int_{\Omega} \vec{F} \cdot \vec{n} dS = 0. \quad (2.5b)$$

We stress that (2.5) is exact and that no approximations have been made to this point.

To illustrate the situation we consider the two-dimensional case shown in Figure 1.

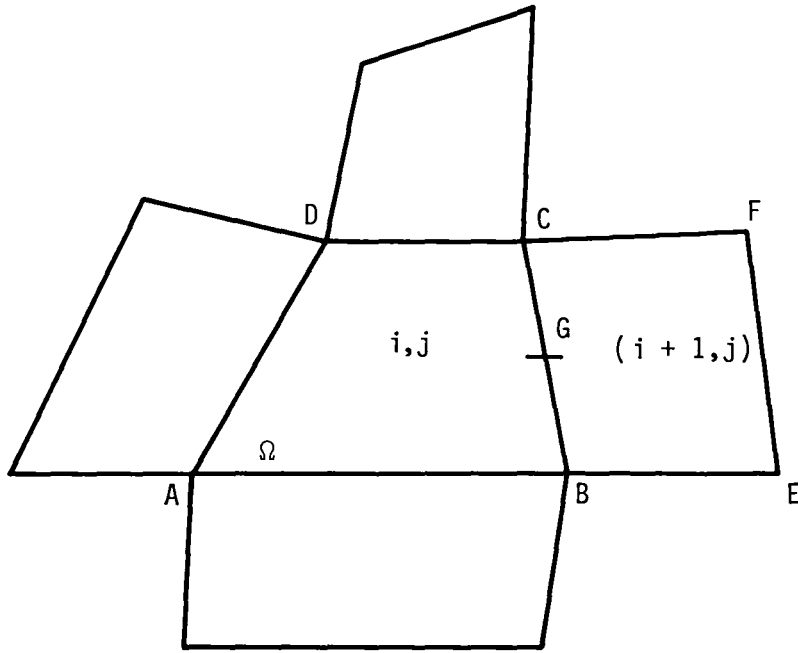


Figure 1

In this case (2.5) becomes

$$\bar{w} = \frac{1}{V} \int_{\Omega} w dx dy \quad (2.6a)$$

$$V \frac{d\bar{w}}{dt} + \int_{AB} + \int_{BC} + \int_{CD} + \int_{DA} (f dy - g dx) = 0. \quad (2.6b)$$

Consider, for example, the integral

$$\int_{BC} f dy - g dx. \quad (2.7)$$

At this stage we replace (2.7) with an integration rule. We would prefer that our formulas be at least second-order accurate for uniform meshes and so we consider two integration rules. The first is the midpoint rule. Thus we have (see Figure 1)

$$\int_{BC} (f dy - g dx) = \Delta y f(G) - \Delta x g(G) + O((\Delta x)^3 + (\Delta y)^3). \quad (2.8)$$

We have replaced the line integral by values of the fluxes at the point G , where G is the midpoint measured in terms of x and y . $\Delta x, \Delta y$ are the changes in x and y respectively between the points B and C . An alternative is to use the trapezoidal rule. We then have

$$\begin{aligned} \int_{BC} f dy - g dx = & \frac{1}{2} [\Delta y (f(B) - f(C)) - \Delta x (g(B) + g(C))] \\ & + O((\Delta x)^3 + (\Delta y)^3). \end{aligned} \quad (2.9)$$

To proceed further we must know the fluxes at the point G (for (2.8)) or B and C (for (2.9)). The fluxes f, g are functions of the dependent variable w and sometimes also the independent variables. However, \bar{w} is defined in (2.6a) as a cell averaged quantity and is not known at specific points. To overcome this difficulty we shall replace \bar{w} by $w_{i,j}$ where $w_{i,j}$ is a point value of w at some point within the cell. An appropriate choice is to use the centroid of the cell and then

$$w_{i,j} = \frac{1}{V} \int_{\Omega} w dv + O(V^2) \quad (2.10)$$

and we retain second-order accuracy.

Having defined $w_{i,j}$ we can then find w at the point G or at B and C by averaging. One possibility (e.g., [8]) is to use simple arithmetic averaging so that

$$w(G) = \frac{1}{2} (w_{i,j} + w_{i+1,j}). \quad (2.11a)$$

Similarly if one uses (2.9) then we have

$$w(C) = 1/4 (w_{i,j} + w_{i+1,j} + w_{i,j+1} + w_{i+1,j+1}). \quad (2.11b)$$

We note that we have averaged the quantity w . Since f and g are nonlinear functions of w we can instead average f and g or else other quantities. The disadvantage of averaging f and g is that this decouples the even and odd points when (2.11a) is used. The advantage of averaging f and g is that in the steady state the fluxes are continuous across shocks if the shock is aligned with a mesh line.

Having made the choice (2.11a) or (2.11b) this completes the space discretization of (2.1). Assuming we average the fluxes the choice of (2.11a) leads to the two-dimensional scheme

$$\begin{aligned} V(\Omega) \frac{dw_{i,j}}{dt} + 1/2 [(f_{i+1,j} + f_{i,j}) \Delta x_{i+1/2,j} - (f_{i,j} + f_{i-1,j}) \Delta x_{i-1/2,j} \\ + (f_{i,j+1} + f_{i,j}) \Delta x_{i,j+1/2} - (f_{i,j} + f_{i,j-1}) \Delta x_{i,j-1/2} \\ + (g_{i+1,j} + g_{i,j}) \Delta y_{i+1/2,j} - (g_{i,j} + g_{i-1,j}) \Delta y_{i-1/2,j} \\ + (g_{i,j+1} + g_{i,j}) \Delta y_{i,j+1/2} - (g_{i,j} + g_{i,j-1}) \Delta y_{i,j-1/2}] = 0 \end{aligned} \quad (2.12)$$

where $V(\Omega) = 1/2 |(y_C - y_A)(x_B - x_D) - (x_C - x_A)(y_B - y_D)|$ (see Figure 1).

Assuming that the positions (x, y) are given at the mesh nodes

$(\Delta x)_{i+1/2,j} = x(C) - x(B)$, etc. For a uniform mesh $\Delta x, \Delta y$ constant this reduces to a centered difference formula

$$\frac{dw_{i,j}}{dt} + \frac{f_{i+1,j} - f_{i-1,j}}{2\Delta x} + \frac{g_{i,j+1} - g_{i,j-1}}{2\Delta y} = 0. \quad (2.13)$$

The trapezoidal rule (2.11b) reduces, in the case of a uniform mesh, to

$$\begin{aligned} \frac{dw_{i,j}}{dt} + 1/4 \left[\frac{f_{i+1,j+1} - f_{i-1,j+1}}{2\Delta x} + 2 \frac{(f_{i+1,j} - f_{i-1,j})}{2\Delta x} + \frac{f_{i+1,j-1} - f_{i-1,j-1}}{2\Delta x} \right. \\ \left. + \frac{g_{i+1,j+1} - g_{i+1,j-1}}{2\Delta y} + 2 \frac{(g_{i,j+1} - g_{i,j-1})}{2\Delta y} + \frac{g_{i-1,j+1} - g_{i-1,j-1}}{2\Delta y} \right] = 0. \end{aligned} \quad (2.14)$$

We shall see later that (2.14) has advantages in terms of the allowable time step and in terms of accuracy, while (2.13) has fewer operations and does not require any special treatment for the tangential components near boundaries.

We will discuss the time integration of these systems later in Section V. For later purposes we note that there is another possibility besides (2.13) and (2.14). This is given by (for uniform meshes)

$$\begin{aligned} \frac{dw_{i,j}}{dt} + 1/2 \left[\frac{f_{i+1,j+1} - f_{i-1,j+1}}{2\Delta x} + \frac{f_{i+1,j-1} - f_{i-1,j-1}}{2\Delta x} \right. \\ \left. + \frac{g_{i+1,j+1} - g_{i+1,j-1}}{2\Delta y} + \frac{g_{i-1,j+1} - g_{i-1,j-1}}{2\Delta y} \right] = 0. \end{aligned} \quad (2.15)$$

We shall see that the stability properties of (2.15) are even better than (2.14) and allow an optimal time step. Now, however the even and odd points are decoupled. In the next section we discuss the accuracy of these schemes.

III. ACCRUACY - ONE DIMENSION

We now consider the accuracy of schemes for nonuniform meshes. To simplify matters we first consider one-dimensional schemes. We consider the equation

$$w_t + f_x = 0. \quad (3.1)$$

We shall also consider the change of variables $\xi = \xi(x)$ and then (3.1) becomes

$$w_t + \frac{f_\xi}{x_\xi} = 0 \quad (3.2a)$$

or in conservation form

$$(x_\xi w)_t + f_\xi = 0. \quad (3.2b)$$

$\xi(x)$ will be chosen so that the nonuniform mesh in x becomes a uniform mesh in ξ . We will usually scale ξ so that $\Delta\xi = 1$. Frequently $\xi(x)$ is never constructed but the variable ξ determines the location of x_j . In one dimension ξ has the property that $\xi(x_j) = j$ at all the nodes, $j = 0, \dots, N$. To construct $\xi(x)$ is now a standard problem in interpolation theory. However, we must have that $\xi'(x_j) \neq 0$ and would prefer that $\xi(x)$ be monotone, i.e., if $x_j \leq x \leq x_{j+1}$ then $j \leq \xi(x) \leq j + 1$. This guarantees that intervals get mapped onto corresponding intervals. In multidimensions we would like to map each cell onto a standard rectangle or cube. If the geometry is so distorted that this cannot be done then this approach is not viable. We stress that there is no need to actually construct ξ and hence there is no need for ξ to be defined globally. Since all accuracy requirements are local, it is sufficient that $\xi(x)$ can be constructed locally at each mesh cell but with sufficient smoothness.

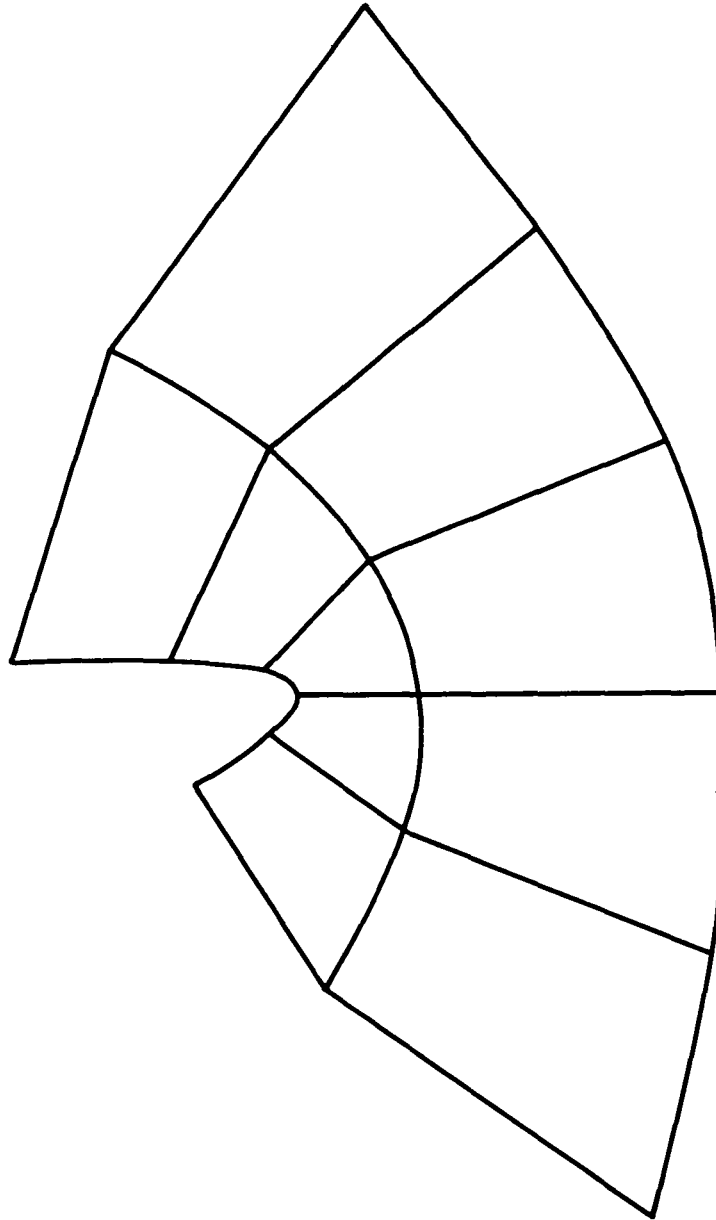


Figure 2

Before discussing accuracy we first mention how nonuniform meshes may be constructed. One difficulty with the analysis is that the theory of accuracy is an asymptotic theory as the mesh is refined. In practice one usually deals with a finite grid which is not extremely fine, especially in three

dimensions. Multidimensional grid generation about general configurations is difficult [16, 17]. Not only is the mesh nonuniform but singularities can appear at which quadrilaterals collapse into triangles. One advantage of a finite volume approach is that the formulas are still valid in this limit. However, it is not clear what happens to the accuracy of the scheme in this degenerate limit. In Figure 2 we show a two-dimensional section of a three-dimensional grid showing a few cells near the leading edge. In the next plane triangular elements appear. This grid was generated using FL057.

Given a mesh there are two ways of constructing a finer mesh. One method is to subdivide each cell into smaller cells. This process usually leads to a smooth distribution but is difficult to implement using general quadrilaterals. An alternative is to grid the entire region anew using more nodes and ignoring the coarser mesh. This is equivalent to refining the mesh in the computational ξ variables. With this method the mesh is less likely to be smooth in the physical space.

Let $r_j = h_{j+1}/h_j$, with h_j the local mesh spacing. We now introduce some notations that govern the rate of stretching.

Definition:

(a) The grid stretching is quasi-uniform (or algebraic) if

$$r_j = 1 + O(h^p), \quad p > 0 \tag{3.3a}$$

$$h = \max_j h_j.$$

We note that the larger p is, the more smooth is the stretching.

(b) The grid stretching is exponential if (a) is not valid but

$$\frac{r_{j+1}}{r_j} = 1 + O(h). \quad (3.3b)$$

(c) The grid stretching rate is faster than exponential if neither (a) nor (b) are true.

We note that (3.3a) can be reformulated as

$$h_{j+1} - h_j = O(h^{p+1}). \quad (3.3a')$$

A typical mesh generator gives an a priori distribution of points in certain directions. Thus, in one space dimension one possibility is

$$x_j = A\kappa^{\alpha j/N} \quad j = 0, 1, \dots, N. \quad (3.4a)$$

Let $h_j = x_j - x_{j-1}$, we then find that

$$\frac{h_{j+1}}{h_j} = \kappa. \quad (3.4b)$$

α and A are chosen so that x_0 and x_N are fixed. Hence

$$A = x_0 \neq 0 \quad (3.4c)$$

$$\alpha = \frac{\log(x_N/x_0)}{\log(\kappa)}. \quad (3.4d)$$

Thus, for fixed $\kappa \neq 1 + O(h)$ we have a fixed ratio between the areas of the cells and so the stretching is exponential. Furthermore, it is shown in [8, 20] that exponential stretchings can accelerate the convergence to a steady state. On the other hand it is shown in [6] that nonuniform meshes may introduce false reflections from the gradients of the stretching. Exponential stretchings are common in many exterior calculations. When $\kappa = 1 + O(h)$ then the stretching is algebraic.

We shall only consider the case that the metric coefficients are evaluated numerically. Hoffman [7] has considered some examples where ξ is a known function of x and all metric derivatives are calculated analytically. He has shown that if Δx is refined so that $\Delta \xi$ is halved then quadratic convergence is retained. This is equivalent to having an algebraic grid stretching.

We wish our formulas to be in conservation form. Again considering the integral form the equation we wish to solve is

$$\frac{d\bar{w}}{dt} + \frac{1}{V} \int_{\Omega} \vec{F} \cdot \vec{n} dS = 0 \quad (3.5a)$$

where \bar{w} is the volume weighted average of w . We say that the scheme is in conservation form if we replace the integral by any consistent approximation. Hence, we replace (2.5) by

$$V_j \frac{d\bar{w}_j}{dt} + \sum_k \alpha_k F_k = 0 \quad (3.5b)$$

where α_k are weights that depend on the nonuniform spacing. In general α_k will depend on several h_j . We must however use the same summation formula in each cell.

We first consider a finite difference mesh where both the dependent variable w_j and the geometric variable x_j are given at the nodes (see Figure 3a).

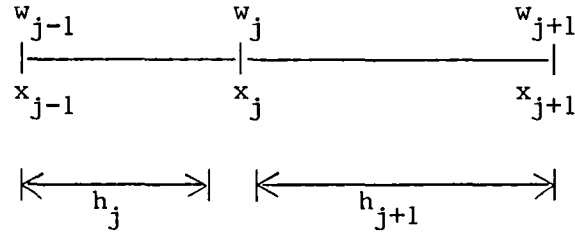


Figure 3a

Let $h_j = x_j - x_{j-1}$. We consider the approximation to (3.1)

Scheme I:

$$\frac{dw_j}{dt} + \alpha_j f_{j-1} + \beta_j f_j + \gamma_j f_{j+1} = 0. \quad (3.6a)$$

By Taylor series we find that this is second-order accurate if

$$\alpha_j = - \frac{h_{j+1}}{h_j(h_j + h_{j+1})} \quad (3.6b)$$

$$\beta_j = \frac{h_{j+1} - h_j}{h_j h_{j+1}} \quad (3.6c)$$

$$\gamma_j = \frac{h_j}{h_{j+1}(h_j + h_{j+1})}. \quad (3.6d)$$

Hence we have

$$\frac{dw_j}{dt} + \frac{h_j}{h_j + h_{j+1}} \left(\frac{f_{j+1} - f_j}{h_{j+1}} \right) + \frac{h_{j+1}}{h_j + h_{j+1}} \left(\frac{f_j - f_{j-1}}{h_j} \right) = 0. \quad (3.6e)$$

However, this scheme is not conservative.

Using the same mesh as in Figure 3a we consider a finite volume scheme. In this case we replace (3.1) with

$$\frac{d}{dt} \int_{x_{j-1}}^{x_{j+1}} w dx + f_{j+1} - f_{j-1} = 0. \quad (3.7)$$

We next approximate the integral by $w_j(x_{j+1} - x_{j-1})$ which is only first-order accurate unless x_j is half way between x_{j-1} and x_{j+1} . We then have

Scheme II:

$$\frac{dw_j}{dt} + \frac{f_{j+1} - f_{j-1}}{x_{j+1} - x_{j-1}} = 0 \quad (3.8a)$$

or in terms of h_j

$$\frac{dw_j}{dt} + \frac{f_{j+1} - f_{j-1}}{h_j + h_{j+1}} = 0. \quad (3.8b)$$

We can also rewrite this scheme in a manner similar to that of (3.6e) as

$$\frac{dw_j}{dt} + \frac{h_{j+1}}{h_j + h_{j+1}} \left(\frac{f_{j+1} - f_j}{h_{j+1}} \right) + \frac{h_j}{h_j + h_{j+1}} \left(\frac{f_j - f_{j-1}}{h_j} \right) = 0. \quad (3.8c)$$

Hence, Scheme II can be interpreted as a volume weighted average of the fluxes at $j - 1/2$ and $j + 1/2$. The flux balance at $j - 1/2$ and $j + 1/2$ are correct to second-order. Nevertheless a Taylor series expansion verifies that this scheme is first-order for a time-dependent problem unless $h_{j+1} - h_j = O(h^2)$, i.e., unless the mesh is quasi-uniform. In a steady state problem we would have to account for a source term or a second dimension so that the problem would be nontrivial. One can have an algorithm that is first-order accurate in space for a time-dependent problem but is second-order accurate in space for a steady state problem. This scheme is also conservative in the sense that

$$\sum_j \left(\frac{h_j + h_{j+1}}{2} \right) w_j$$

is constant except for boundary effects. Thus the conservation takes place if w_j is associated with part of the cell to the left and an appropriate part of the cell to the right of w_j .

We next consider the mapping $\xi = \xi(x)$. A straightforward central differencing to (3.2a) leads to (3.8). We thus conclude that Scheme II is first-order (for nonuniform meshes) in x but is second-order in ξ . In other words, if w is quadratic in ξ then (3.8) is exact but if w is quadratic in x then we have a discretization error. In theory we use a nonuniform mesh because it reflects the gradients of the solution. Hence, it would be natural to assume that w behaves quadratically in ξ rather than in x . In practice the mesh is determined more by geometrical considerations than the behavior of the solution. Furthermore, for a system of equations not all the quantities grow at the same rate. When we are interested in global quantities, e.g., lift and drag, it is not clear if the approximations will be first- or second-order accurate.

We next consider a modification of Scheme II.

Scheme IIa:

$$\frac{dw_j}{dt} + \frac{f_{j+1/2} - f_{j-1/2}}{\kappa_j} = 0 \quad (3.9a)$$

where

$$f_{j+1/2} = \alpha_j f_{j+1} + (1 - \alpha_j) f_j \quad (3.9b)$$

$$\alpha_j = \frac{h_j^2}{h_j^2 + h_{j+1}^2}, \quad h_j = x_j - x_{j-1} \quad (3.9c)$$

$$\kappa_j = \alpha_j h_{j+1} + (1 - \alpha_j) h_j. \quad (3.9d)$$

This scheme uses dependent variables at $j - 1, j, j + 1$ but geometrical data at $j - 2, j - 1, j, j + 1$. A symmetric variant is obtained if (3.9c) is used to define α_{j-1} rather than α_j . One can also obtain a similar formula that depends on the geometrical data at $j - 2$ through $j + 2$. This scheme is second-order in physical space as long as the mesh stretching is no worse than exponential. The scheme is conservative in that $\sum \kappa_j w_j$ is conserved.

We now consider a finite volume scheme where the dependent variables are defined in the center of cells as shown in Figure 3b. This corresponds to the two-dimensional scheme described in the previous section and used in [8].

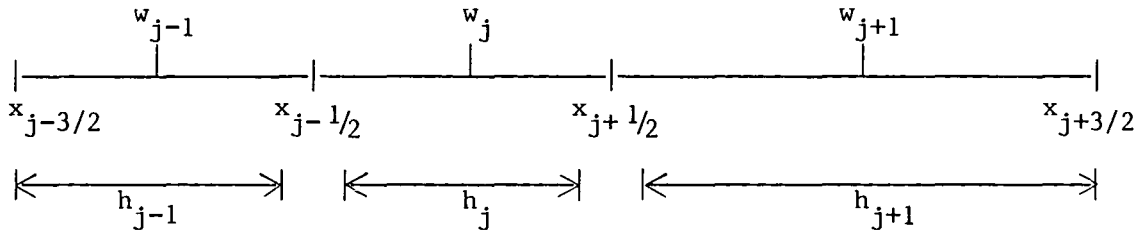


Figure 3b

We then replace (3.1) by

$$\frac{d}{dt} \int_{x_{j-1/2}}^{x_{j+1/2}} w dx + f_{j+1/2} - f_{j-1/2} = 0 \quad (3.10)$$

which as before is exact. Using the procedure described in Section II, e.g. (2.11a), we approximate (3.10) by

$$(x_{j+1/2} - x_{j-1/2}) \frac{dw_j}{dt} + \frac{f_{j+1} + f_j}{2} - \frac{f_j + f_{j-1}}{2} = 0,$$

or

Scheme III:

$$\frac{dw_j}{dt} + \frac{f_{j+1} - f_{j-1}}{2(x_{j+1/2} - x_{j-1/2})} = 0. \quad (3.11)$$

Assuming that f_j is evaluated half way between $x_{j-1/2}$ and $x_{j+1/2}$, a Taylor series expansion verifies that this scheme is inconsistent unless

$$\frac{h_{j+1} - 2h_j + h_{j-1}}{h_j} = 0(h), \quad (3.12)$$

i.e., unless the mesh is quasi-uniform (algebraic) (3.3a). Note that (3.11) is second-order accurate only if the left-hand side of (3.12) is $0(h^2)$, i.e., $r_j = 1 + 0(h^2)$ which requires an even smoother grid, i.e., (3.3a) with $p = 2$. Introducing a mapping $\xi = \xi(x)$ we again verify that (3.11) is second-order in $\Delta\xi$. Hence, we conclude that for an irregular mesh (3.11) is inconsistent in x but is second-order in ξ . However, now the location of w_j is different in the two interpretations. Considering (3.11) in physical space w_j is evaluated half way between $x_{j-1/2}$ and $x_{j+1/2}$, i.e., $x_j = 1/2(x_{j-1/2} + x_{j+1/2})$. However, in ξ space we have $x_j = x(j)$ where $x = x(\xi)$ is the inverse map of $\xi = \xi(x)$, $j - 1/2 = \xi(x_{j-1/2})$, $j + 1/2 = \xi(x_{j+1/2})$. Hence, we assume that $\xi(x)$ is invertible and that if $j - 1/2 \leq \xi \leq j + 1/2$ then $x_{j-1/2} \leq x(\xi) \leq x_{j+1/2}$. Since ξ does not enter into the scheme we only need know that such a $\xi(x)$ exists. The final scheme does not depend on the derivation of (3.11) as coming from a physical or computational space. However, the final interpretation of the numerical solution, e.g., graphics, does depend on how one defines x_j . Furthermore, if the fluxes depend explicitly on the geometry, e.g., cylindrical coordinates, then the two interpretations of (3.11) will result in different schemes.

In order to remove the inconsistency of (3.11) for an exponential mesh we consider another approach previously used by Collela and Woodward to construct upwind differences [5]. Let

$$W(x,t) = \frac{1}{x_{j+1/2} - x_{j-1/2}} \int_{x_{j-1/2}}^x w(x,t) dx. \quad (3.13)$$

Then

$$W(x_{j+1/2}) = w_j \quad (3.14a)$$

is the volume average of w used in the finite volume scheme (3.10). We also have that

$$W(x_{j-1/2}) = 0 \quad (3.14b)$$

$$W(x_{j+3/2}) = w_j + \frac{x_{j+3/2} - x_{j+1/2}}{x_{j+1/2} - x_{j-1/2}} w_{j+1}. \quad (3.14c)$$

The local value of $w(x)$ is then given by $w(x) = \frac{\partial W}{\partial x}$. We now fit $W(x)$ with a quadratic, interpolating at $x_{j-1/2}$, $x_{j+1/2}$, $x_{j+3/2}$ using (3.14). We then differentiate $W(x)$ and evaluate at $x_{j+1/2}$ to find

$$W_{j+1/2} = \frac{h_j W_{j+1} + h_{j+1} W_j}{h_j + h_{j+1}}. \quad (3.15)$$

Then (3.9) becomes

Scheme IIIa:

$$\frac{dW_j}{dt} + \frac{f(W_{j+1/2}) - f(W_{j-1/2})}{x_{j+1/2} - x_{j-1/2}} = 0. \quad (3.16)$$

Interpreting W_j as w at the midpoint between $x_{j-1/2}$ and $x_{j+1/2}$ and expanding in a Taylor series we find that (3.16) has a truncation error

$$\tau = O(h_{j+1} - h_j) + O(h^2).$$

Hence, (3.15), (3.16) is second-order accurate for an algebraic mesh and first-order accurate when used with an exponential mesh. Thus $f_{j+1/2}$ is simply given by linear interpolation in W accounting for the nonuniform mesh. We note that if we wish (3.10) to be fourth-order in space we do not wish to find $f_{j+1/2}$ using cubic interpolation. This occurs since $f_{j+1/2} - f_{j-1/2}$ is only a second-order approximation to $\frac{\partial f}{\partial x}$. Hence, to get fourth-order accuracy we must find $\frac{\partial f}{\partial x}$ directly using x_{j-2} through x_{j+2} . This has been previously observed by Zalesak [23]. We also note that the scheme is conservative since (3.10) is derived from the integral form. In particular

$$\sum_j (x_{j+1/2} - x_{j-1/2}) w_j = \sum_j h_j w_j$$

is constant in time excluding boundary effects. The use of (3.16) gives first-order accuracy if r_j is almost constant, i.e., the mesh is exponential, and gives second-order accuracy if the mesh is algebraic, i.e., $r_j = 1 + O(h)$.

We wish to stress that the difficulties with the cell centered quantities arises because of the finite volume approach. If we define the dependent variables in the center of the cell but use a finite difference approach then we can achieve higher accuracy as was done for the case of nodal variables in Schemes II and IIa. In particular we consider the following generalization of Scheme IIa.

Expanding

$$Q = \frac{1}{\kappa_j} \{ [\alpha_j f_{j+1} + (1 - \alpha_j)f_j] - [\alpha_{j-1} f_j - (1 - \alpha_{j-1})f_{j-1}] \} \quad (3.17)$$

in a Taylor Series we find that

$$\begin{aligned} Q = \frac{1}{\kappa_j} \{ & \frac{1}{2} [\alpha_j (h_j + h_{j+1}) + (1 - \alpha_{j-1})(h_j + h_{j-1})] f' \\ & + \frac{1}{8} [\alpha_j (h_j + h_{j+1})^2 - (1 - \alpha_{j-1})(h_j + h_{j-1})^2] f'' + O(h^3) \}. \end{aligned} \quad (3.18)$$

Hence, Q is a first-order approximation to f' if

$$\kappa_j = \frac{1}{2} [\alpha_j (h_j + h_{j+1}) + (1 - \alpha_{j-1})(h_j + h_{j-1})] + O(h^p), \quad p = 2. \quad (3.19)$$

Furthermore, Q is a second-order approximation if (3.19) holds with $p = 3$ and in addition

$$\alpha_j (h_j + h_{j+1})^2 = (1 - \alpha_{j-1})(h_j + h_{j-1})^2 + O(h^3) \quad (3.20)$$

or letting $r_j = h_{j+1}/h_j$

$$\alpha_j (1 + r_j)^2 = (1 - \alpha_{j-1}) \left(1 + \frac{1}{r_{j-1}}\right)^2 + O(h). \quad (3.20a)$$

For a finite volume scheme $\kappa_j = h_j$ and so (3.19) determines α_j and we have Scheme IIIa which is first-order. For a finite difference scheme we can choose both α_j and κ_j . We thus have

Scheme IIIb:

$$\frac{dw_j}{dt} + \frac{f_{j+1/2} - f_{j-1/2}}{\kappa_j} = 0 \quad (3.21a)$$

$$f_{j+1/2} = \alpha_j f_{j+1} + (1 - \alpha_j) f_j \quad (3.21b)$$

$$\alpha_j = \frac{(h_j + h_{j-1})^2}{(h_j + h_{j-1})^2 + (h_j + h_{j+1})^2}, \quad h_j = x_{j+1/2} - x_{j-1/2} \quad (3.21c)$$

$$\kappa_j = \alpha_j \frac{(h_j + h_{j+1})}{2} + (1 - \alpha_{j-1}) \frac{(h_j + h_{j-1})}{2}. \quad (3.21d)$$

This scheme is now second-order in physical space as long as the mesh spacing is no worse than exponential. However, viewed as a finite volume scheme (3.21a) implies that

$$\int_{x_{j-1/2}}^{x_{j+1/2}} w dx \approx \kappa_j w_j \quad (3.22)$$

which is not within the spirit of a finite volume approach especially for multidimensions.

We now summarize the conclusions of this section. In general both central finite difference formulas and finite volume formulas will be only first-order accurate in the physical variables when nonuniform meshes are used unless the weighted formulas (3.6) are used. When the dependent variables are defined in the middle of the cell then the formulas are not even consistent unless the mesh is quasi-uniform. In most cases the scheme is second-order measured in terms of some computational variables $\xi(x)$. If this variable ξ is carefully chosen to match properties of all components of the solution, then this second-order accuracy is meaningful. However, if the stretching is

utilized simply to put the outer boundary far away then the stretching can reduce the order of accuracy. Numerical experiments verify that the computational solution can be very inaccurate although formally the solution is second-order in ξ . One could possibly post-process the solution, but this would be very difficult to do on general multidimensional meshes.

In this section we have only discussed semidiscrete formulations where the time discretization is not included. It is easy to see that the extensions to fully discrete algorithms using Runge-Kutta type formulas in time, e.g., [8, 20] or else implicit formulas, e.g., [2, 3, 11], are straightforward. When a MacCormack type formula is used then one can again verify that one loses accuracy on a nonuniform grid. In this case to achieve second-order accuracy in x one should let $h_j = x_j - x_{j-1}$ and then

$$\bar{w}_j = w_j^n - \frac{2h_j}{h_j + h_{j+1}} \Delta t \cdot \left(\frac{f_{j+1}^n - f_j^n}{h_{j+1}} \right)$$

(3.23)

and

$$w_j^{n+1} = 1/2 \left[w_j^n + \bar{w}_j - \frac{2h_{j+1}}{h_j + h_{j+1}} \Delta t \left(\frac{\bar{f}_j - \bar{f}_{j-1}}{h_j} \right) \right].$$

IV. ACCURACY - TWO DIMENSIONS

In one dimension we have seen that when the geometrical data and the variables are defined at the same point then a simple averaging of the fluxes gives first-order accuracy in x and second-order accuracy in the computational space variable, ξ . When using nonuniform meshes the accuracy in the physical space can be improved by using the weighted formula (3.6). When the dependent variable is defined in the middle of a cell then simple

averaging of the fluxes can give an inconsistent scheme for an exponentially stretched mesh. Instead a weighted average (3.14), (3.15) should be used.

In extending these results to two space dimensions we encounter several new difficulties. First a x difference at given point i can be given by evaluating it at (i, j) or averaging over several j lines, e.g., (2.13), (2.14), (2.15). In addition weighting formulas, e.g., (3.14), (3.15) must now be replaced by two-dimensional interpolations. By considering cells with equal volume but different shapes it is easy to see that volume weighting can decrease the accuracy of the algorithm. It is necessary to include more information than just the volume of neighboring cells.

In one space dimension we defined a smooth (or quasi-uniform) grid as one for which $r_j = \frac{h_{j+1}}{h_j} = 1 + O(h)$. In two space dimensions we need to consider two-dimensional effects and not just demand that the volumes vary smoothly. Consider the situation shown in Figure 4. All the cells have the same area but it is obvious that one should not define the flux at G as the average of those at the cell centers E and F . Rather the flux at G must be found by a two-dimensional interpolation.

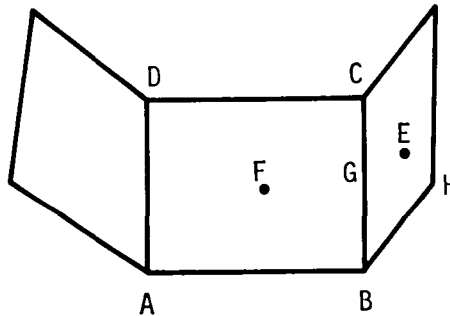


Figure 4

If we wish the standard averaging to be higher order for sufficiently smooth grids, then our notion of smoothness must include changes in angles between zones as well as changes in volumes between zones. We thus define a multidimensional grid as being quasi-uniform if the change between cells of both x and y along each side is small. For example in Figure 4 the grid is quasi-uniform only if

$$\frac{(\Delta x)_{AB}}{(\Delta x)_{BH}} = 1 + O(h) \quad \frac{(\Delta y)_{AB}}{(\Delta y)_{BH}} = 1 + O(h), \quad (4.1)$$

and similarly for the other three sides. It is easy to see that (4.1) holds only when the relative change in both the volume and in the angles is $1 + O(h)$.

We first consider the generalization of Scheme II where the dependent variables and the metrics are defined at the nodes (i, j) . We perform the finite volume integration over the four cells shown in Figure 5.

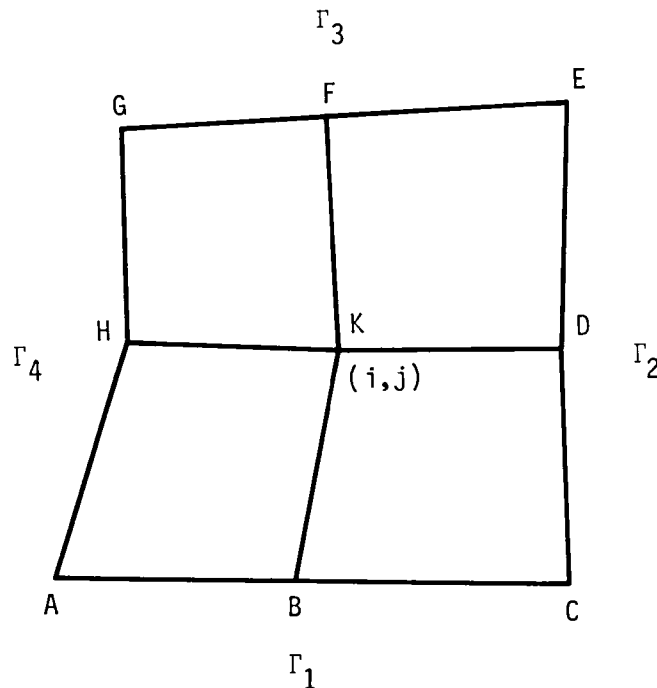


Figure 5

We then have

$$\frac{d}{dt} \iint_{\Omega} w dv + \int_{\Gamma_1 + \Gamma_2 + \Gamma_3 + \Gamma_4} (f dy - g dx) = 0, \quad (4.2)$$

where the line integral is performed in the clockwise direction. We approximate the area integral by $w_{i,j} \cdot V$, where V is the area of the four cells. For the line integrals we can use either the midpoint or trapezoidal rules. The trapezoidal rule is second-order accurate while the midpoint rule is only first-order since $(i + 1, j)$ is not necessarily at the midpoint of Γ_2 . Since the final formula will only be first-order accurate it is not clear if this makes a difference. Using the midpoint we approximate (4.2) by

$$\begin{aligned} \frac{d}{dt} (V(\Omega)w_{i,j}) + f_D \Delta y_{EC} - g_D \Delta x_{EC} - f_F \Delta y_{EC} + g_F \Delta x_{EG} \\ - f_H \Delta y_{GH} + g_H \Delta x_{GA} + f_B \Delta y_{CA} - g_B \Delta x_{CA} = 0 \end{aligned} \quad (4.3)$$

where $V(\Omega) = 1/2 (\Delta y_{EA} \Delta x_{CG} - \Delta x_{EA} \Delta y_{CG})$ and $\Delta x_{CA} = x_C - x_A$ etc.

We see from Figure 5 that H is not necessarily near to being the midpoint of Γ_4 . A better approximation to an integral along Γ_4 is to use the trapezoidal rule on each section. Thus, for example,

$$\int_{\Gamma_4} f dy = \frac{f_G + f_H}{2} (\Delta y)_{HG} + \frac{f_A + f_H}{2} (\Delta y)_{AH}. \quad (4.4)$$

Using a uniform grid (4.3) would reduce to (2.13) while (4.4) would reduce to (2.14). An intermediate possibility is to use the trapezoidal rule on all of Γ_4 . We then would approximate

$$\int_{\Gamma_4} f dy \approx \frac{f_G + f_A}{2} \Delta y_{AG}. \quad (4.5)$$

For a uniform mesh (4.5) would reduce to (2.15). We refer the reader to the appendix for the full two-dimensional formulas.

In this discussion we have not considered the effects caused by the differencing of metrics. In the far field exterior to a body the flow is almost uniform but the mesh is frequently highly stretched. It is desirable that the derivatives be small independent of the mesh stretching. Steger [14] discusses various techniques to accomplish this. It is obvious that finite volume schemes automatically satisfy this grid conservation property, see, e.g., (A2), (A4). In addition Steger also presents numerous examples that demonstrate the effect of nonuniform or highly skewed grids on the accuracy of the solution. For some schemes highly stretched meshes can also affect the rate of convergence to a steady state.

V. TIME INTEGRATION

All the formulas discussed until this point have used a semidiscrete formulation and have concentrated on the space discretization. One possible way of integrating these equations in time is to use an implicit method with A.D.I. splitting for multidimensional problems (see [2], [3]). In the rest of this section we shall describe and analyze the use of Runge-Kutta type formulas [8].

Let L_u represent the space discretization of a method. Then a K stage Runge-Kutta method has the form

$$u^{(1)} = u^n + \alpha_1 \Delta t L u^n \tag{5.1}$$

$$u^{(k)} = u^n + \alpha_k \Delta t L u^{(k-1)} \quad k = 1, 2, \dots, K$$

where $u^{n+1} = u^{(K)}$. $\alpha_1, \dots, \alpha_K$ are given parameters with $\alpha_K = 1$ for at least first-order accuracy in time. When L has constant coefficients we can Fourier transform (5.1). Let $Q(\theta, \psi)$ be the Fourier transform of the space discretization operator L and let \hat{u} be the Fourier transform of u . We then find that (5.1) becomes

$$\hat{u}^{n+1} = G \hat{u}^n \tag{5.2a}$$

where

$$G = P_K(\hat{Q} \Delta t) \tag{5.2b}$$

and P_K is a polynomial

$$P_K(z) = \sum_{j=0}^K \beta_j z^j \tag{5.2c}$$

where

$$\beta_0 = 1, \beta_1 = \alpha_K, \beta_j = \alpha_K \alpha_{K-1} \dots \alpha_{K-j+1}. \tag{5.2d}$$

(5.2c) generates a stability region, i.e., a domain in the complex plane where $|P_K(z)| \leq 1$. We shall now consider the hyperbolic (inviscid) case. All the formulas introduced have central differences and so Q lies on the imaginary axis. In this case (5.1) is stable if

$$\Delta t \leq \frac{K}{\lambda} \tag{5.3}$$

where K depends on the sequence $\alpha_1, \dots, \alpha_K$ and

$$\lambda = \max_{-\pi \leq \theta, \psi \leq \pi} \rho(\hat{Q}(\theta, \psi)) \quad (5.4)$$

where $\rho(\hat{Q})$ is the spectral radius of \hat{Q} . Hence, given a sequence $\alpha_1, \dots, \alpha_K$ the allowable time step depends on the eigenvalues of \hat{Q} , i.e., on properties of the scheme.

Specifically we consider the Euler equations in general curvilinear coordinates. This system can be written as

$$w_t + Aw_x + Bw_y = 0 \quad (5.5)$$

where (x, y) are general coordinates $w = (\rho, \rho u, \rho v, E)^t$ and

$$A = \begin{pmatrix} 0 & Y_y & -X_y & 0 \\ Y_y s^2 - uq & q - (\gamma-2)Y_y u & -X_y u - (\gamma-1)Y_y v & (\gamma-1)Y_y \\ -X_x s^2 - vq & Y_y v + (\gamma-1)X_x u & q + (\gamma-1)X_x v & -(\gamma-1)X_x \\ -q(h-s^1) & Y_y h - (\gamma-1)qu & -X_y h - (\gamma-1)qv & \gamma q \end{pmatrix} \quad (5.6)$$

$$B = \begin{pmatrix} 0 & -Y_x & X_x & 0 \\ -Y_x s^2 - ur & r + (\gamma-2)Y_x u & X_x u + (\gamma-1)Y_x v & -(\gamma-1)Y_x \\ X_x s^2 - vr & -Y_x v - (\gamma-1)X_x u & r - (\gamma-2)X_x v & (\gamma-1)X_x \\ -r(h-s^2) & -Y_x h - (\gamma-1)ru & X_x h - (\gamma-1)rv & \gamma r \end{pmatrix} .$$

Here X, Y are the Cartesian coordinates and (x, y) are the generalized coordinates. Also

$$q = Y_y u - X_y v$$

$$r = X_x v - Y_x u$$

(5.7)

$$s^2 = \frac{(\gamma - 1)}{2} (u^2 + v^2)$$

$$h = \frac{c_2}{\gamma - 1} + \frac{u^2 + v^2}{2} .$$

We first consider the case that

$$f_x \approx \frac{f_{i+1,j} - f_{i-1,j}}{2\Delta x} , \quad g_y \approx \frac{g_{i,j+1} - g_{i,j-1}}{2\Delta y} . \quad (5.8)$$

This scheme (2.11a) is used in FL052, [8] and reduces to (2.13) for a uniform mesh. In this case the stability criterion becomes [20]

$$\Delta t \leq \frac{K}{|q| + |r| + \sqrt{X_x^2 + Y_x^2 + X_y^2 + Y_y^2} + 2|X_x X_y + Y_x Y_y|c} . \quad (5.9)$$

We next consider the case where the flux integrals are approximated by the trapezoidal rule. This scheme is given in (2.11b) and reduces to (2.14) for a uniform mesh. The schemes given in the appendix, which account for nonuniformities in the mesh while averaging, are also included in this case. We thus consider

$$f_x \approx \frac{f_{i+1,j+1} - f_{i-1,j+1} + 2(f_{i+1,j} - f_{i-1,j}) + f_{i+1,j-1} - f_{i-1,j-1}}{8\Delta x} \quad (5.10)$$

$$g_y \approx \frac{g_{i+1,j+1} - g_{i+1,j-1} + 2(g_{i,j+1} - g_{i,j-1}) + g_{i-1,j+1} - g_{i-1,j-1}}{8\Delta y} .$$

For this case the stability limit is given by [19]

$$\Delta t \leq \frac{K}{|w| + \sqrt{a^2 + b^2} c} \quad (5.11)$$

with

$$a = \frac{Y_x + Y_y + \max(Y_x, Y_y)}{2} ,$$

$$b = \frac{X_x + X_y + \max(X_x, X_y)}{2} \quad (5.12)$$

$$w = \frac{q + r + \max(q, r)}{2} .$$

We note that this is a larger time step than allowed by (5.9) but at the expense of a more complicated algorithm. In FL052 the calculation of the fluxes and the artificial viscosity accounts for most of the running time. Hence, complicating the averaging procedure for the fluxes does not require much extra computer time.

Finally we consider the averaging

$$f_x \approx \frac{(f_{i+1,j+1} - f_{i-1,j+1}) + (f_{i+1,j-1} - f_{i-1,j-1})}{4\Delta x} \quad (5.13)$$

$$g_y \approx \frac{(g_{i+1,j+1} - g_{i+1,j-1}) + (g_{i-1,j+1} - g_{i-1,j-1})}{4\Delta y} .$$

In this case we can give two criteria that are sufficient for stability (see also [1]). One is that

$$\Delta t \leq K \max \left[\frac{\Delta x}{\rho(A)}, \frac{\Delta y}{\rho(B)} \right] \quad (5.14)$$

or equivalently

$$\Delta t \leq \frac{K}{\max \left[|q| + \sqrt{X_y^2 + Y_y^2} c, |r| + \sqrt{X_x^2 + Y_x^2} c \right]} \quad (5.15)$$

This is the same condition one would obtain using time splitting. A second possible criterion is that

$$\Delta t \leq \frac{K}{\max(|q|, |r|) + \sqrt{\max(X_x^2 + X_y^2, Y_x^2 + Y_y^2)} c} \quad (5.16)$$

Both these criteria provide sufficient conditions for stability. In both cases these allow larger time steps than (5.11) which in turn allow larger time steps than (5.9).

VI. STABILITY

We next consider the effect of a nonuniform grid on the stability of an explicit scheme. To be specific we will compare the Schemes III and IIIa for the one-dimensional problem. For an equation with constant coefficients

$$w_t + aw_x = 0$$

Scheme III (3.10) becomes

$$\frac{dw_j}{dt} + Qw = 0 \quad (6.1a)$$

with

$$Qw_j = \frac{a(w_{j+1} - w_{j-1})}{2(x_{j+1/2} - x_{j-1/2})} \quad (6.1b)$$

Formally replacing w_j by $e^{ij\xi}$ (i.e., forming the pseudodifference operator) we find that

$$\hat{Q} = \frac{ai}{x_{j+1/2} - x_{j-1/2}} \cdot \sin \xi. \quad (6.2)$$

We thus see that the symbol is purely imaginary. Using a Runge-Kutta type scheme [8] (see also (5.1)-(5.4)), this leads to a stability limit of the form

$$\frac{h_j}{\Delta t_j} = \frac{x_{j+1/2} - x_{j-1/2}}{\Delta t_j} \leq K/a \quad (6.3)$$

where K is given by the intersection of the stability curve of the Runge-Kutta scheme with the imaginary axis.

We next consider the Scheme IIIa (3.14)-(3.15) with constant coefficients,

$$\frac{dw_j}{dt} + Q_a w = 0 \quad (6.4a)$$

where

$$Q_a w_j = \frac{a}{h_j} \left(\frac{h_j w_{j+1} + h_{j+1} w_j}{h_j + h_{j+1}} - \frac{h_{j-1} w_j + h_j w_{j-1}}{h_{j-1} + h_j} \right). \quad (6.4b)$$

In this case

$$\begin{aligned} \hat{Q}_a = \frac{a}{h_j} & \left[\frac{h_j (h_{j+1} - h_{j-1})}{(h_j + h_{j+1})(h_{j-1} + h_j)} (1 - \cos \xi) \right. \\ & \left. + i \left(1 + \frac{h_j^2 - h_{j-1} h_{j+1}}{(h_j + h_{j+1})(h_{j-1} + h_j)} \right) \sin \xi \right] \xi. \end{aligned} \quad (6.5)$$

Note: \hat{Q}_a has a nonzero real part. \hat{Q}_a is dissipative if and only if

$$a(h_{j+1} - h_{j-1}) \geq 0. \quad (6.6)$$

In other words, if the mesh expands in the direction of the wave then the wave is dissipated. If the mesh contracts in the direction of the wave motion then the wave is amplified. Alternatively, consider an O mesh where the spacing between nodes increases as the mesh goes to the outer boundary. Then outgoing waves are dissipated while incoming waves are amplified. Thus absorbing boundary conditions are important. We point out that the above statement is not completely accurate. The stability region of many Runge-Kutta schemes include a portion of the positive complex plane. Hence, even though the real part of $-\hat{Q}$ is positive, nevertheless, the total Runge-Kutta scheme can be dissipative. Usually this intrusion of the stability region into the right half plane is largest near the imaginary stability limit. Hence, the amplification of incoming waves is least pernicious when the time step is near the stability limit. This is an additional motivation to use a local time step.

The time step restriction for (6.5) is much more difficult to analyze than for (6.2) since \hat{Q} contains real and imaginary parts that depend on the Fourier variable ξ . As before we let $r_j = h_{j+1}/h_j$, then

$$\hat{Q}_a = \frac{a}{h_j} \left[\frac{r_j r_{j-1} - 1}{(1 + r_j)(1 + r_{j-1})} (1 - \cos \xi) + i \left(1 + \frac{r_{j-1} - r_j}{(1 + r_j)(1 + r_{j-1})} \right) \sin \xi \right]. \quad (6.7)$$

Hence, if the mesh is algebraic then $\hat{Q}_a = \hat{Q} + O(h)$ and so the stability limit is given by (6.3). When the mesh ratio is exponential then the imaginary part of \hat{Q} (i.e., the wave speed) is changed by $O(1)$ terms. Hence, for an exponentially stretched mesh the stability properties of the scheme are different than that for a uniform mesh.

In this entire analysis we have assumed that the coarsest mesh is still sufficiently fine to resolve the waves. Hence, stability analysis, which is an asymptotic theory, is still valid. In many cases the outer meshes are large compared with the relevant wave lengths. In this case other phenomena, e.g., wave reflections, may also be present, see [6].

We next consider the effect of using a local time step for the fully discrete algorithm. (6.1) can then be approximated by

$$W_j^{n+1} - W_j^n + \frac{a\Delta t_j}{2(x_{j+1/2} - x_{j-1/2})} (W_{j+1}^n - W_{j-1}^n) = 0 \quad (6.8)$$

choosing $\Delta t_j = K(x_{j+1/2} - x_{j-1/2})$ as the local time step (6.8) becomes

$$W_j^{n+1} - W_j^n + \frac{K}{2} (W_{j+1}^n - W_{j-1}^n) = 0 \quad (6.9)$$

which is stable when used in a Runge-Kutta type mode for the appropriate K .

However, now all effects of the nonuniform mesh disappear. Hence, in one dimension we have recovered the standard analysis. Thus using a local time step removes the dissipation or growth previously discussed. It also removes the false reflection found by Giles and Thompson [6]. Using the finite volume scheme with linear interpolation, (6.4), the use of a local time step cannot remove the real part of the eigenvalues and so we cannot recover the properties of a uniform grid.

VII. COMPUTATIONAL RESULTS

In order to show the value of accounting for the nonuniform mesh we present one sample case. We consider the Runge-Kutta scheme for the Euler equations, FL052T described in [8]. This is a finite volume method with the unknowns given at the cell centers. As a specific case we consider the two-dimensional flow about a NACA0012. The inflow conditions are $M_\infty = 0.3$, $\alpha = 10^\circ$. Since this is a subsonic flow the numerical solution can be compared with the solution to a potential code with a very fine mesh. In Table I we present the lift and drag for a coarse $64 \times 16 \times 0$ mesh. The original code is based on a two-dimensional version of (3.9)-(3.10) while the new version is based on (3.14)-(3.15). Though this correction only accounts for one-dimensional effects we note a marked improvement in the results.

Table I

Code	C_L	C_D
Potential code with fine mesh	1.274	0.0000
Original FL052T $64 \times 16 \times 0$ mesh	1.227	0.0087
Improved version	1.264	0.0025

Comparison of new and original code for flow about NACA0012 with $M_\infty = 0.3$, $\alpha = 10^\circ$.

VIII. CONCLUSION

In (3.3) we defined algebraic and exponential rates of grid stretching. With an algebraic stretching, the grid metrics are sufficiently smooth that all second-order techniques retain their formal accuracy. When exponential or faster stretching is used then the accuracy of a central difference scheme or finite volume method will deteriorate to first-order accuracy unless special weighting formulas are used, e.g., (3.6). When the dependent variables are defined at the center of the cells, then the finite volume approach can yield an inconsistent scheme unless the weighting (3.14) is used. With this weighting the scheme is second-order for an algebraic stretching and is first-order when the stretching is faster than algebraic.

In all cases the algorithm is second-order measured in terms of a computational variable ξ rather than in terms of the physical coordinate x . If this ξ corresponds to the behavior of all components of the solution, then this measure of accuracy is reasonable. It is clear that ξ should always be chosen so that the solution is smooth in the ξ variable. However, in many cases ξ is chosen simply to put the outer boundary sufficiently far away. Thus, for example, if the solution has a boundary layer then one would want the grid to be almost uniform within the boundary layer. One could use an exponential mesh in the outer region only if the solution decays exponentially in the far field. Furthermore, if $\xi = \xi(x)$ is not given analytically but rather x_j is given then there may not exist a sufficiently smooth and monotone $\xi(x)$.

In multidimensions these difficulties are compounded. First the grid is quasi-uniform only if both the volumes and all angles vary sufficiently slowly. Difficulties in constructing multidimensional grids leads to

nonuniform grids that are due to geometrical effects that have nothing to do with the behavior of the solution, e.g, Figure 2. Hence, in this case, it becomes more important to introduce weights that compensate for the nonuniform grid. Unfortunately the weighting formulas must now account for the multidimensional geometrical behavior. One possibility is to use bilinear interpolation within a cell as is done in finite element codes, see formulas in the appendix.

In several dimensions the line integrals of the fluxes can be approximated by either a midpoint or a trapezoidal rule. For a uniform mesh with cell centered variables the midpoint rule yields a simpler formula and one that gives no difficulty for the tangential flux near a boundary. However, when the mesh is distorted the midpoint rule may be more inaccurate due to difficulties in locating the actual midpoint. Furthermore, if a two-dimensional interpolation is used then the simplicity of the midpoint rule is lost. The trapezoidal rule requires more work but allows a larger time step. In addition it is now easier to use either volume weighting or bilinear interpolation to calculate the value of the fluxes at the nodes. Weighting formulas similar to (3.14) can now be used; see the appendix for full two-dimensional formulas. Alternatively one can use a finite difference or finite volume scheme where all variables are defined at the nodes. This guarantees first-order accuracy in x even when the mesh is exponential. For two-dimensional problems, grids can be constructed which are fairly quasi-uniform. In this case both approaches give similar accuracy, see, e.g., [17]. For three-dimensional problems about complex bodies it is much more difficult to construct a quasi-uniform grid. In this case some sort of patching of grids may be necessary.

The use of a trapezoidal integration rule instead of the midpoint rule allows a larger time step but at the expense of a slightly more complicated formula and additional difficulties near the boundaries. The use of weighted formulas can change the dissipation and stability properties of the scheme.

We also show that nonuniform meshes may change the dissipation properties of the time integration scheme. These dissipation terms are further changed if a local time step is used.

APPENDIX

In this appendix we give the details for two separate two-dimensional schemes. The extension to three dimensions is immediate. We only consider the semidiscrete problem with the time integration to be explicit Runge-Kutta or else some implicit scheme.

In the first algorithm we assume that both the coordinates and variables are given at the nodes (see Figure A1). We use a finite volume approach and evaluate the line integrals using a trapezoidal rule.

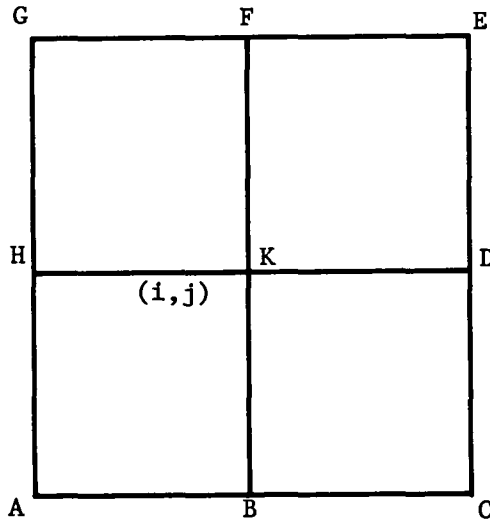


Figure A1

Consider the equation

$$w_t + f_x + g_y = 0. \tag{A1}$$

We convert this to an integral relationship as in (2.6). Let f_A denote f at the point A and let $\Delta x_{B+1} = x_B - x_H$ etc. for all the possibilities. Note that the order of the indices is important. We then have

Scheme A1:

$$\begin{aligned}
 v_{ij} \frac{dw_{i,j}}{dt} + 1/2 [& f_A \Delta y_{BH} + f_B \Delta y_{CA} + f_C \Delta y_{DB} + f_D \Delta y_{EC} \\
 & + f_E \Delta y_{FD} + f_F \Delta y_{GE} + f_G \Delta y_{HF} + f_H \Delta y_{AG}] \\
 & - 1/2 [g_A \Delta x_{BH} + g_B \Delta x_{CA} + g_C \Delta x_{DB} + g_D \Delta x_{EC} \\
 & + g_E \Delta x_{FD} + g_F \Delta x_{GE} + g_G \Delta x_{HF} + g_H \Delta x_{AG}] = 0
 \end{aligned} \tag{A2}$$

where

$$v_{i,j} = 1/2 |\Delta y_{EA} \Delta x_{CG} - \Delta x_{EA} \Delta y_{CG}|.$$

For a uniform Cartesian mesh this reduces to

$$\begin{aligned}
 \frac{dw_{i,j}}{dt} + \frac{f_C - f_A + 2(f_D - f_H) + f_E - f_G}{4\Delta x} \\
 + \frac{g_G - g_A + 2(g_F - g_B) + g_E - g_C}{4\Delta y} = 0.
 \end{aligned} \tag{A3}$$

The second scheme that we consider has the geometrical quantities at the nodes but the dependent variables are given at the cell centers (see Figure A2) this extends the scheme used in FL052 [8]. However, we use the trapezoidal rule to evaluate the integrals rather than the midpoint rule used in [8].

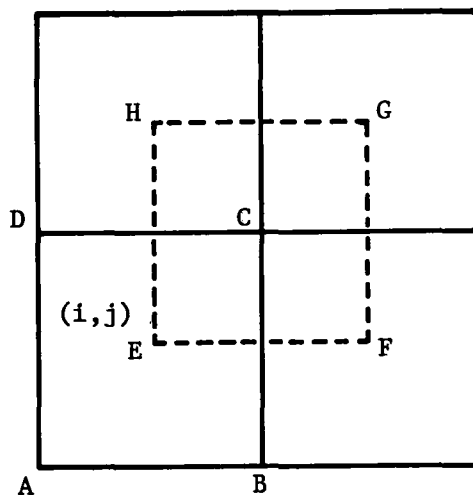


Figure A2

The results in

Scheme A2:

$$v_{i,j} \frac{dw_{i,j}}{dt} + 1/2 [(f_C - f_A)\Delta y_{DB} + (f_B - f_D)\Delta y_{CA}]$$

(A4)

$$- 1/2 [(g_C - g_A)\Delta x_{DB} + (g_B - g_D)\Delta x_{CA}] = 0.$$

In order to evaluate the fluxes at the nodes we could use volume weighted averages. An alternative is to use bilinear interpolation using the cell centers. We first must locate the cell centers. Using simple averaging we find that

$$x_{i,j} = 1/4 (x_A + x_B + x_C + x_D)$$

(A5)

$$y_{i,j} = 1/4 (y_A + y_B + y_C + y_D).$$

As an example of using bilinear interpolation we give the formulas for calculating f at the point C given the values of f at the points $E, F, G,$ and H and given the locations of all the nodes and cell centers. Let

$$G_1 = (f_{i+1,j} - f_{i,j})\Delta x_{GE} - (f_{i+1,j+1} - f_{i,j})\Delta x_{FE}$$

$$G_2 = (f_{i+1,j} - f_{i,j})\Delta x_{HE} - (f_{i,j+1} - f_{i,j})\Delta x_{FE}$$

$$\alpha = \Delta y_{FE} \Delta x_{GE} - \Delta y_{GE} \Delta x_{FE}$$

(A6)

$$\beta = (x_{i+1,j} y_{i+1,j} - x_{i,j} y_{i,j})\Delta x_{GE} - (x_{i+1,j+1} y_{i+1,j+1} - x_{i,j} y_{i,j})\Delta x_{FE}$$

$$\gamma = \Delta y_{FE} \Delta x_{HE} - \Delta y_{HE} \Delta x_{FE}$$

$$\delta = (x_{i+1,j} y_{i+1,j} - x_{i,j} y_{i,j})\Delta x_{HE} - (x_{i,j+1} y_{i,j+1} - x_{i,j} y_{i,j})\Delta x_{FE}.$$

We then define

$$C = \frac{\delta G_1 - \beta G_2}{\alpha \delta - \beta \gamma}, \quad D = \frac{\alpha G_2 - \gamma G_1}{\alpha \delta - \beta \gamma}$$

$$B = \frac{f_{i+1,j} - f_{i,j} - C\Delta y_{FE} - D(x_{i+1,j} y_{i+1,j} - x_{i,j} y_{i,j})}{\Delta x_{FE}} \quad (A7)$$

$$A = f_{i,j} - Bx_{i,j} - Cy_{i,j} - Dx_{i,j} y_{i,j}.$$

Finally we have

$$f_C = A + Bx_C + Cy_C + Dx_C y_C. \quad (A8)$$

For a uniform mesh $\Delta x = \Delta y$ this gives

$$f_C = 1/4 (f_{i,j} + f_{i+1,j} + f_{i,j+1} + f_{i+1,j+1}). \quad (A9)$$

For both Scheme A1 and Scheme A2 the stability condition is given by (5.11). This allows a larger time step than the stability criterion (5.9) for the scheme used in FL052.

Acknowledgement

The author would like to thank A. Bayliss and S. Yaniv for many fruitful discussions.

REFERENCES

- [1] Abarbanel, S. and D. Gottlieb, A note on the leap-frog scheme in two and three dimensions, J. Comput. Phys., 21 (1976), pp. 351-355.

- [2] Beam, R. W. and R. F. Warming, An implicit finite difference algorithm for hyperbolic systems in conservation law form, J. Comput. Phys., 22 (1976), pp. 87-110.

- [3] Briley, W. R. and H. McDonald, Solution of the multidimensional compressible Navier-Stokes equations by a generalized implicit method, J. Comput. Phys., 24 (1977), pp. 372-397.

- [4] Clarke, D. K., M. D. Salas, and H. A. Hassan, Euler calculations for multi-element airfoils using Cartesian grids, AIAA 85-0291.

- [5] Colella, P. and P. R. Woodward, The piecewise-parabolic method (PPM) for gas dynamical calculations, J. Comput. Phys., 54 (1984) pp. 174-201.

- [6] Giles, M. and W. T. Thompkins, Jr., Interval reflection due to a nonuniform grid, Advances in Computer Methods for Partial Differential Equations V (IMACS), (R. Vichnevetsky and R. S. Stepleman, eds.), 1984, pp. 322-328.

- [7] Hoffman, J. D., Relationship between the truncation errors of centered finite difference approximation on uniform and nonuniform meshes, J. Comput. Phys., 46 (1982), pp. 469-474.

- [8] Jameson, A., W. Schmidt, and E. Turkel, Numerical solutions of the Euler equations by finite volume methods using Runge-Kutta time-stepping schemes, AIAA 81-1259.

- [9] Mastin, C. W., Error induced by coordinate systems, Numerical Grid Generation, (J. F. Thompson, ed.), Elsevier-North Holland, Amsterdam, 1982, pp. 31-40.

- [10] Pike, T., Grid adaptive algorithms for the solution of the Euler equations on irregular grids, J. Comput. Phys., to appear, 1985.

- [11] Pullman, T. H. and J. L. Steger, Recent improvements in efficiency, accuracy, and convergence for implicit approximate factorization algorithms, AIAA 85-0360.

- [12] Rai, M. M., K. A. Hennesius, and S. R. Chakravarthy, Metric discontinuous zonal grid calculations using the Osher scheme, Comput. & Fluids, 12 (1984), pp. 161-176.

- [13] South, J. C., Recent advances in computational transonic aerodynamics, AIAA 85-0366.

- [14] Steger, J. L., On application of body conforming curvilinear grids for finite difference solution of external flow, Numerical Grid Generation (J. F. Thompson, ed.) Elsevier-North Holland, Amsterdam, 1982, pp. 295-316.

- [15] Swanson, R. C. and E. Turkel, A multistage time-stepping scheme for the Navier-Stokes equations, AIAA 85-0035.

- [16] Thompson, J. F., U. A. Warsi, and C. W. Mastin, Boundary-fitted coordinate systems for numerical solution of partial differential equations - a review, J. Comput. Phys., 47 (1982), pp. 1-108.

- [17] Thompson, J. F., A survey of grid generation techniques in computational fluid dynamics, AIAA 83-0447.

- [18] Thompson, J. F., A survey of dynamically adaptive grids in the numerical solution of partial differential equations, Appl. Numer. Math., 1 (1984), pp. 3-27.

- [19] Turkel, E., Composite methods for hyperbolic equations, SIAM J. Numer. Anal., 14 (1977), pp. 744-759.

- [20] Turkel, E., Acceleration to a steady state for the Euler equations, Proc. INRIA Euler Workshop, (SIAM), 1983.

- [21] Turkel, E., Algorithms for the Euler and Navier-Stokes equations for supercomputers, The Impact of Supercomputers in the Next Decade of CFD, Birkhauser, Boston, 1984.

- [22] Vinokur, M., On one-dimensional stretching functions for finite difference calculations, J. Comput. Phys., 50, (1983), pp. 215-234.

- [23] Zalesak, S. T., Fully multidimensional flux-corrected transport algorithms for fluids, J. Comput. Phys., 31 (1979), pp. 335-362.

End of Document